J|A|C|S
COMMUNICATIONS

Spectroscopic Characterization of YedY: The Role of Sulfur Coordination in a Mo(V) Sulfite Oxidase Family Enzyme Form

Jing Yang,† Richard Rothery,‡ Joseph Sempombe,† Joel H. Weiner,‡ and Martin L. Kirk*,†

Department of Chemistry and Chemical Biology, The University of New Mexico, Albuquerque, New Mexico 87131, and Department of Biochemistry, 474 Medical Science Building, University of Alberta, Edmonton, Alberta T6G 2H7, Canada

Received April 25, 2009; E-mail: mkirk@unm.edu

The pyranopterin molybdenum enzymes are commonly grouped into the sulfite oxidase, DMSO reductase, and xanthine oxidase families on the basis of the type of reactions they catalyze, their active-site structures, and the nature of the overall protein fold.[1] Members of the sulfite oxidase (SO) enzyme family possess a common SUOX protein fold and include vertebrate and plant SO (PSO), the sulfite dehydrogenase from *Starkeya novella* (SDH), assimilatory nitrate reductases, and bacterial YedY.[2] High-resolution crystal structures, coupled with the results of resonance Raman and electron paramagnetic resonance (EPR) studies, are consistent with the active-site structures shown in Figure 1. The sulfite-oxidizing enzymes catalyze the oxidation of sulfite to sulfate, which is the terminal step in the degradation of sulfur-containing amino acids and various other sulfur-containing chemicals. The catalytic reaction represents a two-electron oxidation of the substrate coupled to an oxygen atom transfer. Under turnover conditions, the paramagnetic Mo(V) form represents an obligatory catalytic intermediate in the electron transfer (ET) regeneration of the catalytically competent active site and is therefore of considerable mechanistic importance. Although the d^1 Mo(V) state in SO family enzymes has been studied extensively by paramagnetic resonance spectroscopies, optical spectroscopies have been extremely limited because of the presence of highly absorbing heme (vertebrate SO and SDH) or the difficulty in preparing large quantities of Mo(V) resulting from unfavorable Mo(VI)/(V) and Mo(V)/(IV) redox couples (PSO).[3,4] EPR redox titrations indicate that YedY possesses neither of these problems, allowing electronic spectra of a Mo(V) center belonging to an SO family protein to be obtained for the first time.[5]

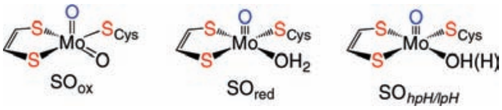

Figure 1. Accepted oxidized (SO_{ox}), reduced (SO_{red}), and Mo(V) pH-dependent ($SO_{hpH/lpH}$) active-site structures for SO family enzymes. It should be noted that the average $O_{oxo}-Mo-S_{Cys}-C$ dihedral angles are 80° for CSO and 65° for YedY.

Very recently, the crystal structure of YedY was solved at 2.5 Å resolution.[6] The structure revealed that YedY is a monomeric SUOX fold protein with no other cofactors and a Mo domain that is remarkably similar to that found in chicken SO (CSO),[7] *Arabidopsis thaliana* PSO,[8,9] and SDH.[10] Furthermore, the coordination geometry of the Mo active site in YedY is virtually identical to that determined for other members of the SO family, although significant differences in the substrate binding pocket, namely, the absence of charged arginine residues, suggest that YedY does not effectively bind anionic substrates. The putative reductase activity of YedY is supported by activity assays and kinetic data on a number of oxidizing substrates.[6] As-isolated YedY exists primarily in the paramagnetic Mo(V) oxidation state, which allows detailed spectroscopic probing of the Mo(V) form by a combination of electronic absorption, magnetic circular dichroism (MCD), and EPR spectroscopies. The work described here details the first such combined optical and EPR spectroscopic characterization of a Mo(V) SO family enzyme form. This provides the basis for correlating EPR-derived spin Hamiltonian parameters, the nature of charge-transfer (CT) bands in the electronic spectra, and the active-site structures of YedY and other members of the SO family.

The low-temperature (50 K) anisotropic X-band EPR spectrum of YedY is presented in Figure 2. Spectral simulations yield spin Hamiltonian parameters that differ from those reported for SDH, PSO, and CSO.[11−13] Specifically, the **g** and **A** tensors are highly axial in YedY, and a *very* large g_1 is observed. Single-crystal EPR studies on monooxomolybdenum model complexes indicate that the largest primary component of the hyperfine tensor (i.e., A_1) is oriented very close to the Mo≡O bond. For YedY, the noncoincidence angles indicate that g_1 is rotated 19.5° from A_1, and this is very similar to the angles of 14 and 18° found for the *hpH* and *lpH* forms of CSO. Although rotations of g_1 relative to A_1 have been correlated to Mo−X (X = F, Cl, Br) bond covalency in C_s-symmetric Tp^*MoOX_2 model compounds,[14] no such correlation has been observed in lower-symmetry complexes or the enzymes. The large g_1 for YedY deserves comment, as it is even larger than g_1 for the *very rapid* xanthine oxidase intermediate (XO_{vr}).[15] This is important, as XO possesses a terminal sulfido ligand in place of

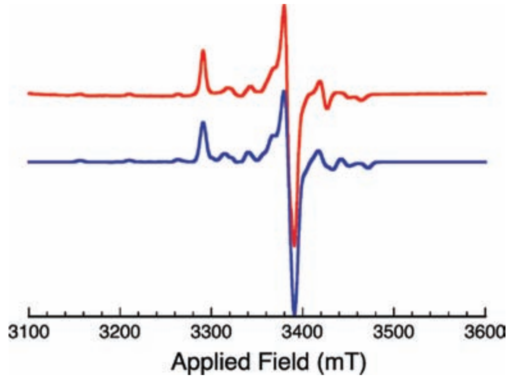

Figure 2. X-band EPR spectrum of as-isolated YedY at 50 K (red). The spectral simulation (blue) yields $g_1 = 2.030$, $g_2 = 1.974$, $g_3 = 1.969$, $A_1 = 54.5 \times 10^{-4}$ cm^{-1}, $A_2 = 23.5 \times 10^{-4}$ cm^{-1}, and $A_3 = 22.5 \times 10^{-4}$ cm^{-1}, with Euler angles $\alpha = 35.5°$, $\beta = 19.5°$, and $\gamma = -46.0°$. It should be noted that the highly axial nature of the YedY EPR spectrum results in a large degree of uncertainty in α and γ.

---

† The University of New Mexico.
‡ University of Alberta.

10.1021/ja903087k CCC: $40.75

the S_{Cys} donor found in members of the SO family, and the highly covalent $Mo{=}S_{sulfido}$ d−p π^* bonding scheme[16] in XO is believed to be responsible for the large value of g_1 in XO_{vr}. Thus, an increase in $Mo(x^2{-}y^2){-}S$ covalency is the likely origin for the larger g_1 observed in YedY. Both $Mo(x^2{-}y^2){-}S_{dithiolene}$ and $Mo(x^2{-}y^2){-}S_{Cys}$ sulfur covalency contributions are anticipated to increase g_1.[17] We have shown that deviations from an $O_{oxo}{-}Mo{-}S_{thiolate}{-}C$ dihedral angle of 90° lead to an increase in $Mo(x^2{-}y^2){-}S^{v}$ covalency (see Figure 3) in monooxomolybdenum thiolate model complexes.[18−20] In contrast, the $Mo(x^2{-}y^2){-}S^{\sigma}$ contribution is anticipated to possess a minimal $O_{oxo}{-}Mo{-}S_{Cys}{-}C$ dihedral angle dependence, as this is a σ-bonding interaction. Therefore, second coordination sphere effects in YedY that involve the $O_{oxo}{-}Mo{-}S_{Cys}{-}C$ dihedral angle may lead to the observed increase in g_1 via an increase in the $Mo(x^2{-}y^2){-}S^{v}$ bonding interaction.[21] Alternatively, a large dithiolene chelate ring folding about the ligand S···S vector may lead to an increase in g_1.[22−25]

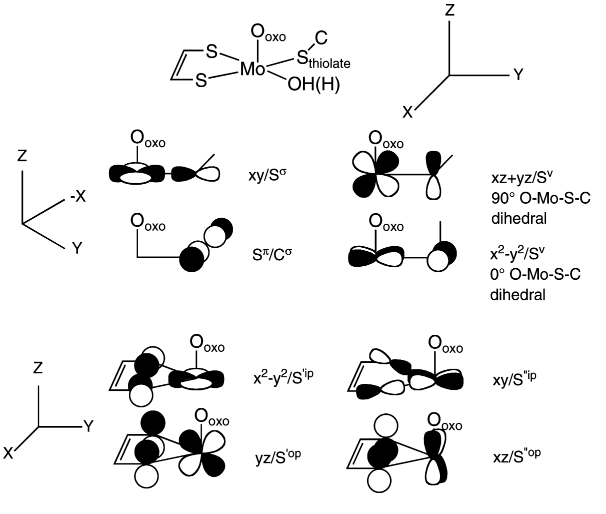

Figure 3. Symmetrized (top) Mo−thiolate and (bottom) Mo−dithiolene bonding interactions in YedY.

Pink-colored YedY equilibrated in pH 7 buffer (20 mM MOPS, 500 mM NaCl, 20 mM histidine) displays absorption features at 11 825 cm^{-1} (ε = 125 M^{-1} cm^{-1}), 19 550 cm^{-1} (ε = 612 M^{-1} cm^{-1}), and 27 425 cm^{-1} (ε = 1600 M^{-1} cm^{-1}) (Figure 4). Gaussian resolution of the electronic absorption spectrum, coupled with MCD data, provide evidence for a total of at least six electronic transitions below ∼30 000 cm^{-1} in YedY. A combination of molecular orbital (MO) theory, transition-state calculations using time-dependent density functional theory (DFT) methods,[26,27] and similarities to spectral features of oxomolybdenum dithiolene and thiolate model complexes have allowed us to understand the electronic origin of the three lowest-energy ligand-to-metal CT (LMCT) transitions in YedY.

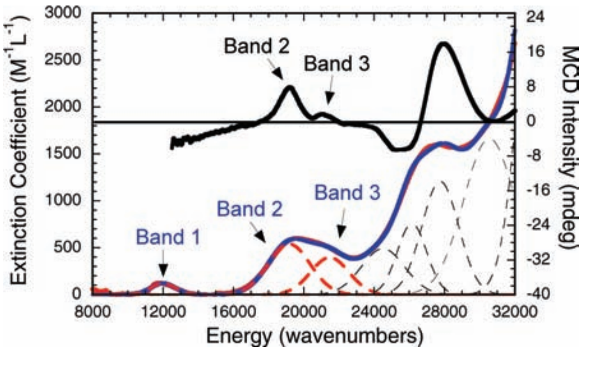

Figure 4. As-isolated YedY MCD spectra at 7 T and 5 K (black) and electronic absorption spectra at 300 K (blue). Gaussian resolution of the absorption spectrum is shown as dashed lines, and the composite spectrum is presented as a red line. Electronic absorption data have been corrected for background Rayleigh scattering.

The highest occupied β MO (β-HOMO) in oxomolybdenum monodithiolenes is a dithiolene-based MO comprising two S atomic orbitals that are out-of-plane (op) with respect to the dithiolene plane and in-phase with one another (S'^{op}; Figure 3). Additionally, the lowest-energy acceptor orbital in these complexes is the in-plane (ip) $Mo(x^2{-}y^2)$ lowest unoccupied β MO (β-LUMO). This acceptor orbital experiences a large stabilization relative to the $Mo(xz,yz)$ orbital set of t_{2g} parentage as a result of the strong π^* interaction between the $Mo(xz,yz)$ orbitals and the terminal oxo ligand.[28] A similar bonding scheme is anticipated for YedY. We therefore assign band 1 as the $S'^{op} \rightarrow Mo(x^2{-}y^2)$ LMCT transition (β-HOMO → β-LUMO) on the basis of this MO scheme and the assignment of a similar transition at ∼9000 cm^{-1} in Tp*MoO(bdt) (bdt = benzene-1,2-dithiolate) and related complexes.[28] Band 2 is assigned as the cysteine thiolate $S^{v}{}_{Cys} \rightarrow Mo(x^2{-}y^2)$ transition (β-HOMO-1 → β-LUMO) on the basis of spectral assignments in oxomolybdenum thiolate model compounds.[18−20,29] The orientation of the $S^{v}{}_{Cys}$ p orbital is orthogonal to the $Mo{-}S_{Cys}$ bond, and both the degree of $S^{v}{}_{Cys}{-}Mo(x^2{-}y^2)$ orbital overlap and the intensity of the $S^{v}{}_{Cys} \rightarrow Mo(x^2{-}y^2)$ CT transition are related to the $O_{oxo}{-}Mo{-}S^{v}{}_{Cys}{-}C$ dihedral angle.[18] We note that the $S'^{op} \rightarrow Mo(x^2{-}y^2)$ and $S^{v}{}_{Cys} \rightarrow Mo(x^2{-}y^2)$ transitions in YedY occur at energies that are ∼3000 cm^{-1} higher than those observed in the model systems. Band 3 is formally the $Mo(x^2{-}y^2) \rightarrow Mo(xz{+}yz)$ ligand-field transition and would be expected to possess a very low oscillator strength. However, because of a large exchange-mediated stabilization of the majority-spin $Mo(x^2{-}y^2)$ orbital (α-HOMO-1), there is considerable thiolate character (31% S^{v}) mixed into the α-HOMO-1 wave function.[26,27] Thus, the primary intensity-gaining mechanism is $S^{v}{}_{Cys} \rightarrow Mo(xz{+}yz)$, and the transition may be viewed as LMCT in nature (α-HOMO-1 → α-LUMO+1). A summary of these band assignments is presented in Table 1.

Table 1. Electronic Absorption and MCD Band Assignments

band	E^{soln}_{max} (cm^{-1})	oscillator strength (exptl/calcd)	E^{MCD}_{max} (cm^{-1})	assignment
1	11 900	0.0009/0.0003	n.d.	$S'^{op} \rightarrow Mo(x^2{-}y^2)$
2	19 122	0.0069/0.0044	19 289	$S^{v}{}_{Cys} \rightarrow Mo(x^2{-}y^2)$
3	21 578	0.0047/0.0033	21 026	$Mo(x^2{-}y^2) + S^{v}{}_{Cys} \rightarrow Mo(xz{+}yz)$

The spectroscopic data for YedY provide insight into how the coordinated dithiolene and cysteine thiolate conspire to modulate the Mo reduction potential and provide a putative hole superexchange pathway for ET regeneration of the dioxomolybdenum(VI) active site in sulfite-oxidizing enzymes. The low intensity of the $S'^{op} \rightarrow Mo(x^2{-}y^2)$ transition indicates very poor $S'^{op}{-}Mo(x^2{-}y^2)$ orbital overlap, which may result from the small amount (∼2.5°) of dithiolene chelate ring folding about the S···S vector[22−25] observed in the crystal structure of YedY. Thus, the lack of an appreciable "sulfur fold" effectively decouples the S^{op} dithiolene orbital from the $Mo(x^2{-}y^2)$ redox orbital. This precludes the involvement of the S'^{op} orbital, either directly or via mixing with the S'^{ip} orbital, in ET processes at this geometry unless ligand redox processes (i.e., the pyranopterin dithiolene) are operative.

The greater intensity of Band 2 indicates an appreciable degree of cysteine thiolate character mixed into the $Mo(x^2{-}y^2)$ β-LUMO.

Our earlier work on oxomolybdenum thiolates[18] indicates that Mo(x^2-y^2)$-$S^v covalency contributions are minimized when the O$_{oxo}$$-Mo-S_{thiolate}$$-$C dihedral angle, x, is 90° and vary as

$$\% \mathrm{S^v} \text{ character} = \cos^2(x) \times 25 \qquad (1)$$

Using this expression and the 65° O$_{oxo}$$-Mo-S_{Cys}$$-$C dihedral angle found in YedY, we obtain an estimate of 4.5% $\mathrm{S^v}_{Cys}$ character in the YedY β-LUMO wave function, which is in good agreement with the value calculated for the active site using DFT (5.9%).[26,27]

Although the O$_{oxo}$$-Mo-S_{Cys}$$-$C dihedral angle ranges from 72 to 80° in structurally characterized sulfite-oxidizing enzymes, their *hpH* and *lpH* g_i values are essentially identical. Thus, in apparent contrast to the structural data, the EPR parameters imply very similar structures for the Mo(V) oxidation state. We have shown that the optimized structure for a computational model of these active sites yields an O$_{oxo}$$-Mo-S_{Cys}$$-$C dihedral angle of 80°,[30] in excellent agreement with the crystallographically determined CSO geometry. According to eq 1, an 80° dihedral angle results in ~0.75% $\mathrm{S^v}_{Cys}$ character in the CSO β-LUMO wave function. Thus, the increased value of g_1 and the more acute O$_{oxo}$$-Mo-S_{Cys}$$-$C dihedral angle observed in the structure of YedY strongly support an ~6-fold increase in YedY Mo(x^2-y^2)$-$$\mathrm{S^v}_{Cys}$ covalency relative to Mo(V) forms of CSO, PSO, and SDH. Our calculations also indicate that the presence of an aqua ligand, as opposed to a hydroxide, can yield g_1 values greater than 2.0 via an increase in Mo$-$S covalency. These factors may be at least partially responsible for the increased stability of the Mo(V) state and the observed reductase activity in YedY relative to other sulfite-oxidizing enzymes.[6] Additional dithiolene S^{op}$-$Mo(*xz*,*yz*) and cysteine S^v$-$Mo(*xz*,*yz*) bonding interactions could further modulate the reduction potential of the active site through anisotropic ligand-to-metal charge donation,[19,25,31] and this would be expected to facilitate a decrease in hard-donor stabilization of a dioxo Mo(VI) active site.

In conclusion, we have made initial spectral assignments for the lowest-energy optical transitions in YedY using a combination of electronic absorption, MCD, and EPR spectroscopies. Importantly, the results indicate that the S^{op} → Mo(x^2-y^2) transition is markedly weaker than the cysteine thiolate → Mo(x^2-y^2) CT band, and this reflects dominant cysteine sulfur covalency contributions to the Mo(x^2-y^2) β-LUMO wave function at the YedY active-site geometry. This is consistent with a minimal folding of the dithiolene chelate ring in YedY and a more acute O$_{oxo}$$-Mo-S_{Cys}$$-$C dihedral angle than in the Mo(V) forms of CSO, PSO, and SDH. The observation of a more acute O$_{oxo}$$-Mo-S_{Cys}$$-$C dihedral angle in YedY results in increased S^v → Mo(x^2-y^2) CT, which is the likely origin of the large g_1 observed in the EPR spectrum of YedY. Since both S$_{Cys}$ → Mo and S$_{dithiolene}$ → Mo CT bands are observed in YedY, the relative thiolate and dithiolene covalency contributions can be probed as a function of specific active-site mutations and substrate/inhibitor binding and directly correlated to EPR data. Finally, the spectrosocopic results presented here, coupled with available structural data, indicate that second coordination sphere effects (i.e., dithiolene chelate ring folding, changes in cysteine thiolate dihedral angles, charge differences surrounding the active site, solvent access) may play key roles in modulating the active-site redox potential, facilitating ET regeneration, and affecting the type of reactions catalyzed by SO family enzymes.

Acknowledgment. M.L.K. acknowledges support from the National Institutes of Health (Grant GM-057378). J.H.W. acknowledges support from the Canadian Institutes of Health Research (Grant MOP15292).

Supporting Information Available: Complete ref 27, details of the bonding calculations, MOs involved in the lowest-energy LMCT transitions, and a table of Mo enzyme spin Hamiltonian parameters. This material is available free of charge via the Internet at http://pubs.acs.org.

References

(1) Hille, R. *Chem. Rev.* **1996**, *96*, 2757.
(2) Workun, G. J.; Moquin, K.; Rothery, R. A.; Weiner, J. H. *Microbiol. Mol. Biol. Rev.* **2008**, *72*, 228.
(3) Helton, M. E.; Pacheco, A.; McMaster, J.; Enemark, J. H.; Kirk, M. L. *J. Inorg. Biochem.* **2000**, *80*, 227.
(4) Jones, R. M.; Inscore, F. E.; Hille, R.; Kirk, M. L. *Inorg. Chem.* **1999**, *38*, 4963.
(5) Brokx, S. J.; Rothery, R. A.; Zhang, G. J.; Ng, D. P.; Weiner, J. H. *Biochemistry* **2005**, *44*, 10339.
(6) Loschi, L.; Brokx, S. J.; Hills, T. L.; Zhang, G.; Bertero, M. G.; Lovering, A. L.; Weiner, J. H.; Strynadka, N. C. J. *J. Biol. Chem.* **2004**, *279*, 50391.
(7) Kisker, C.; Schindelin, H.; Pacheco, A.; Wehbi, W. A.; Garrett, R. M.; Rajagopalan, K. V.; Enemark, J. H.; Rees, D. C. *Cell* **1997**, *91*, 973.
(8) Hille, R. *Structure* **2003**, *11*, 1189.
(9) Schrader, N.; Fischer, K.; Theis, K.; Mendel, R. R.; Schwarz, G.; Kisker, C. *Structure* **2003**, *11*, 1251.
(10) Kappler, U.; Bailey, S. *J. Biol. Chem.* **2005**, *280*, 24999.
(11) Kappler, U.; Bailey, S.; Feng, C. J.; Honeychurch, M. J.; Hanson, G. R.; Bernhardt, P. V.; Tollin, G.; Enemark, J. H. *Biochemistry* **2006**, *45*, 9696.
(12) Hemann, C.; Hood, B. L.; Fulton, M.; Hansch, R.; Schwarz, G.; Mendel, R. R.; Kirk, M. L.; Hille, R. *J. Am. Chem. Soc.* **2005**, *127*, 16567.
(13) Lamy, M. T.; Gutteridge, S.; Bray, R. C. *Biochem. J.* **1980**, *185*, 397.
(14) Nipales, N. S.; Westmoreland, T. D. *Inorg. Chem.* **1997**, *36*, 756.
(15) Wilson, G. L.; Greenwood, R. J.; Pilbrow, J. R.; Spence, J. T.; Wedd, A. G. *J. Am. Chem. Soc.* **1991**, *113*, 6803.
(16) Doonan, C. J.; Rubie, N. D.; Peariso, K.; Harris, H. H.; Knottenbelt, S. Z.; George, G. N.; Young, C. G.; Kirk, M. L. *J. Am. Chem. Soc.* **2008**, *130*, 55.
(17) Drew, S. C.; Hill, J. P.; Lane, I.; Hanson, G. R.; Gable, R. W.; Young, C. G. *Inorg. Chem.* **2007**, *46*, 2373.
(18) Peariso, K.; Helton, M. E.; Duesler, E. N.; Shadle, S. E.; Kirk, M. L. *Inorg. Chem.* **2007**, *46*, 1259.
(19) McNaughton, R. L.; Helton, M. E.; Cosper, M. M.; Enemark, J. H.; Kirk, M. L. *Inorg. Chem.* **2004**, *43*, 1625.
(20) McNaughton, R. L.; Tipton, A. A.; Rubie, N. D.; Conry, R. R.; Kirk, M. L. *Inorg. Chem.* **2000**, *39*, 5697.
(21) Peariso, K.; Chohan, B. S.; Carrano, C. J.; Kirk, M. L. *Inorg. Chem.* **2003**, *42*, 6194.
(22) Inscore, F. E.; Joshi, H. K.; McElhaney, A. E.; Enemark, J. H. *Inorg. Chim. Acta* **2002**, *331*, 246.
(23) Joshi, H. K.; Cooney, J. J. A.; Inscore, F. E.; Gruhn, N. E.; Lichtenberger, D. L.; Enemark, J. H. *Proc. Natl. Acad. Sci. U. S. A.* **2003**, *100*, 3719.
(24) Inscore, F. E.; Knottenbelt, S. Z.; Rubie, N. D.; Joshi, H. K.; Kirk, M. L.; Enemark, J. H. *Inorg. Chem.* **2006**, *45*, 967.
(25) Kirk, M. L.; Helton, M. E.; McNaughton, R. L. *Prog. Inorg. Chem.* **2004**, *52*, 111.
(26) MOs were analyzed using the AOMix program: (a) Gorelsky, S. I. *AOMix: Program for Molecular Orbital Analysis*; York University: Toronto, 1997. (b) Gorelsky, S. I.; Lever, A. B. P. *J. Organomet. Chem.* **2001**, *635*, 187.
(27) Frisch, M. J.; et al. *Gaussian 03*, revision C.02; Gaussian, Inc.: Wallingford, CT, 2004.
(28) Inscore, F. E.; McNaughton, R.; Westcott, B. L.; Helton, M. E.; Jones, R.; Dhawan, I. K.; Enemark, J. H.; Kirk, M. L. *Inorg. Chem.* **1999**, *38*, 1401.
(29) McMaster, J.; Carducci, M. D.; Yang, Y. S.; Solomon, E. I.; Enemark, J. H. *Inorg. Chem.* **2001**, *40*, 687.
(30) Peariso, K.; McNaughton, R. L.; Kirk, M. L. *J. Am. Chem. Soc.* **2002**, *124*, 9006.
(31) Holm, R. H.; Kennepohl, P.; Solomon, E. I. *Chem. Rev.* **1996**, *96*, 2239.

JA903087K